NTP ASSISTED SINGLE STEP METHANE CONVERSION TO METHANOL OVER Cu/γ-AL$_2$O$_3$ CATALYST MODIFIED BY ZnO, ZrO$_2$ AND MgO AS PROMOTERS

A Dissertation Submitted to

Indian Institute of Technology Hyderabad

in Partial Fulfillment of the Requirements for The Degree of

MASTER OF SCIENCE

By

DHEERAJ KUMAR

(CY16MSCST11006)

Under the Supervision of

Prof.Ch. Subrahmanyam

भारतीय प्रौद्योगिकी संस्थान हैदराबाद
Indian Institute of Technology Hyderabad

DEPARTMENT OF CHEMISTRY

INDIAN INSTITUTE OF TECHNOLOGY HYDERABAD

INDIA

MAY 2018

Declaration

I declare that this written submission represents my ideas in my own words, and where others' ideas or words have been included, I have adequately cited and referenced the original sources. I also declare that I have adhered to all principles of academic honesty and integrity and have not misrepresented or fabricated or falsified any idea/data/fact/source in my submission. I understand that any violation of the above will be a cause for disciplinary action by the Institute and can also evoke penal action from the sources that have thus not been properly cited, or from whom proper permission has not been taken when needed.
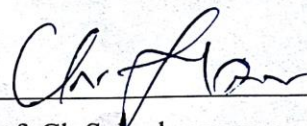
Signature)

Dheeraj Kumar

cy16mscst11006

Approval Sheet

This thesis entitled NTP assisted single step methane conversion to methanol over different promoters by Dheeraj Kumar is approved for the degree of Master of Science from IIT Hyderabad.

Prof. Ch.Subrahmanyam

Dr.Surendra Kumar Martha

Dr. M.Deepa

Acknowledgements

First and top tier I would like to thank Prof. Ch.Subrahmanyam my supervisor for taking me as a student and helping me in academically and personally. Over the last one year I have learnt a lot of things from him and I am glad that my institute had given me chance to work with him. I appreciate him for encouraging my project and helping me to complete it smoothly. It was really a great honor and learning process for me to work under his guidance.

As an M.Sc student project success would have been impossible without an excellent group member. I am very grateful for all the members of my lab for both social and professional interactions.

I like to appreciate and thank PhD scholar Ms. Piu Chawdhury for her constant help and support, Mr. Debjyoti Ray and Mr. Devadutta Nepak for his advices and motivation. I am extremely grateful to my other lab mates for their encouragement in learning experimental techniques and their helpful thoughts in my project work.

I am very much thankful to the Department of Chemistry at IIT Hyderabad to provide the instrumental facilities, for which I have completed my project at given time.
Finally, I must thank to all my friends and family for always keeping me motivated, without this I may never have finished writing.

Dedicated

to

My parents, Mr. Dinesh Kumar Singh and Mrs. Gita Devi

My Brother Manohar Singh

Abstract

Methane, a potential greenhouse gas can be converted to an alternative fuel, methanol in a single step by NTP-DBD reactor at ambient condition through high energy electron impact, where air was used as an oxidant. Present experiment employs a plasma-catalyst combination system to trap the synergy condition due to catalyst action and uniform surface discharge. The influence of the reaction condition (power, CH_4 /Air mole ratio) and supported metal catalysts was investigated in terms of the conversion of the feed gases, selectivity and yield of the products and the energy efficiency of the plasma process. During the present study, $CuO/\gamma-Al_2O_3$ and modified by metal oxides (ZnO, ZrO_2 and MgO) catalysts were prepared by impregnation as the promoter modification leads to the high dispersion of the small metal particles over support material and hence improves the catalytic activity. Compared to the non-catalytic plasma reaction, combination of plasma-catalyst system gave reliable increment on both CH4 conversion and CH_3OH selectivity. The highest CH_4 conversion of ~11% obtained from CMgA catalyst and the highest methanol selectivity of 28.3% obtained from CZrA catalyst.

TABLE OF CONTENTS

LIST OF ABBREVIATIONS

DBD: Dielectric Barrier Discharge

IPCC: Intergovernmental Panel on Climate Change

CLTE: Complete Local Thermodynamic Equilibrium

PLTE: Partial Local Thermodynamic Equilibrium

OES: Optical Emission Spectroscopy

TEM: Transmission Electron Microscope

SEM: Scanning Electron Microscope

CCP: Capactively Coupled Plasma

MPOM: Methane Partial Oxidation to Methanol

XRD: X-Ray Diffraction

CA: CuO/Al_2O_3

CZnA: $CuO/ZnO/Al_2O_3$

CZrA: $CuO/ZrO_2/Al_2O_3$

CMgA: $CuO/MgO/Al_2O_3$

EDS: Energy-Dispersive X-Ray Spectroscopy

SAED: Selected Area Electron Diffraction

BET: Brunauer–Emmett–Teller

JCPDS: Joint Committee On Powder Diffraction Standards

SIE: Specific Input Energy

CHAPTER 1
INTRODUCTION

1.1. Prolegomenon

Energy is the single most influential resource that shepherd the development of a given country [1]. Fossil fuels is the most accessible source of energy nowadays but excessive use of it making it decline due to its overall fixed amount in nature. The conversion of fossil fuels into energy has severe environmental and health implications. Discussions of global warming often summon passionate responses and savage debate between members to different views of the threat posed [2].

By-products formed during the combustion of fossil fuels lead to the world's most significant threat to children's health and future and are major contributors to environmental injustice and global inequality [1-2]. By products consist of divers of air pollutants, CO_2 and natural gas which are the most disastrous and climate-altering greenhouse gases. Synergies between air pollution and climate change can magnify the harm to human beings. Impacts include impairment of cognitive and behavioural development, respiratory illness, and other chronic diseases.

Therefore, we need sustainable source which can remove these disadvantages and fulfil our requirements. Methanol is one source of fuel which is clean and renewable [3]. It can be used in many other process and in industries for many purpose. But the production of methanol in conventional process need a very harsh condition. Many new processes are being developed to increase its productivity and decrease the cost of production.

1.2. Global Warming

Global warming is a highly controversial and debated topic for many scientist, ecologist and even for the common man. It means the temperature raise of the earth, due to absorption of sunlight (infrared radiation) by some gases like Ozone (O_3), carbon dioxide (CO_2), hydrofluorocarbons (HFCs), perfluorocarbons (PFCs), and sulphur hexafluoride (SF_6), methane (CH_4), water vapour and nitrous oxide (N_2O). these gases do not let whole sunlight to go to the atmosphere again but some part is absorbed by these gases which slowly and slowly increase the earth temperature. It is disturbing our whole ecosystem and results like melting of glaciers, climate change, rise in sea level etc. Due to the burning of fossil fuels many of these gases are released and disturb the environment. Methane is major component of natural gases and one of the major responsible gases for greenhouse effect [4]. Although CH4 emission is

smaller than that of CO_2, but it has a tendency to absorb and release IR radiation, which results an increase in worlds temperature on a continuous basis due to the formation of a thermal layer in the atmosphere. Actually, CH_4 has a 25 times larger potential impact to trap heat than CO_2 on increasing global warming. New research in the journal Nature indicates that for each degree that the Earth's temperature rises, the amount of methane entering the atmosphere from microorganisms dwelling in lake sediment and freshwater will increase several times. As temperatures rise, the relative increase of methane emissions will outpace that of carbon dioxide from these sources, the researchers report [5].
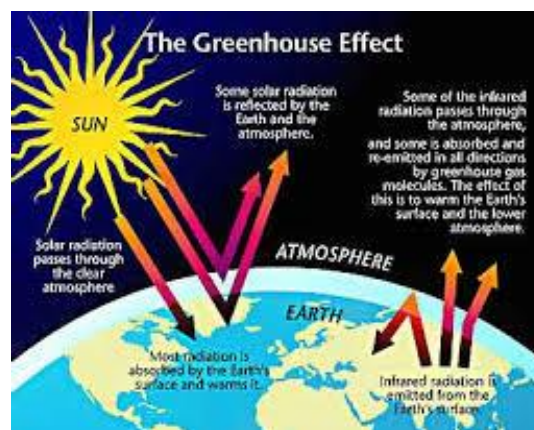

Fig 1: Schematic representation of greenhouse effect.

1.3. Methane emission sources

Methane is a colourless odourless gas. It is also known as marsh gas or methyl hydride. It is easily ignited. The vapours are lighter than air. Methane is produced by the breakdown or decay of organic material and can be introduced into the atmosphere by either natural processes – such as the decay of plant material in wetlands, the seepage of gas from underground deposits or the digestion of food by cattle or human activities such as oil and gas production, rice farming or waste management[6].Major sources and sinks of present-day methane emission and their relative contribution to the global methane balance demonstrate great uncertainties in the identification and quantification of individual sources and sinks. Most recent methane projections of the Intergovernmental Panel on Climate Change (IPCC) for 2025 and 2100 are discussed and used to estimate the contribution of population growth to future methane emission [6-7].
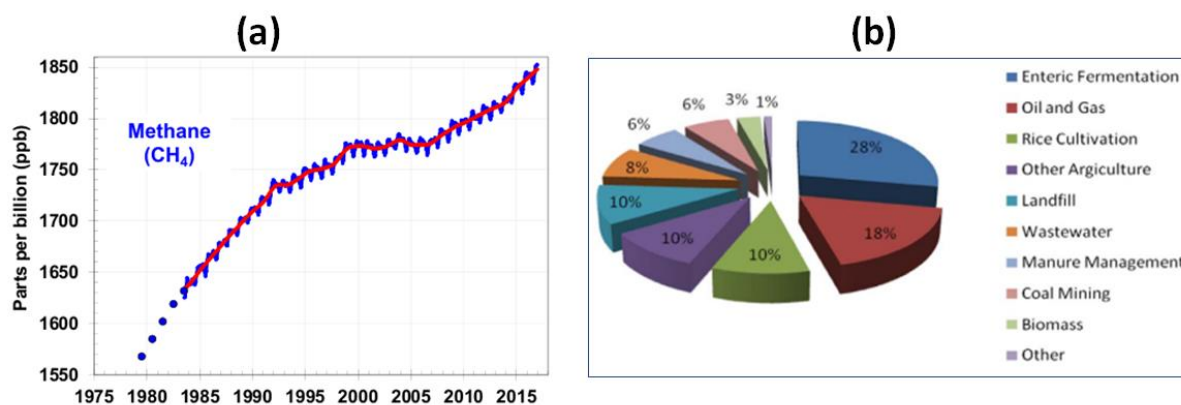
Fig. 2. (a) CH4 emission rate (b) Anthropogenic source of CH₄.

1.4. **Production of methanol**

The methanol industry spans the entire globe, with production in Asia, North and South America, Europe, Africa and the Middle East. Worldwide, over 90 methanol plants have a combined production capacity of about 110 million metric tons (almost 36.6 billion gallons or 138 billion litres). According to IHS, global methanol demand reached 70 million metric tons in 2015 (23 billion gallons/87 billion litres), driven in large part emerging energy applications for methanol which now account for 40% of methanol consumption. Each day, nearly 200,000 tons of methanol is used as a chemical feedstock or as a transportation fuel (67 million gallons/254 million litres). That's enough methanol every day to fill nearly 7,500 tanker trucks stretching end-to-end for 63 miles or 100 kilometres [8].

Fig. 3. Methanol economy.

1. 5. Uses of methanol

12

Methanol is an essential chemical widely used in various purposes. But some major uses are as follows: -

- *Reagent in several processes*
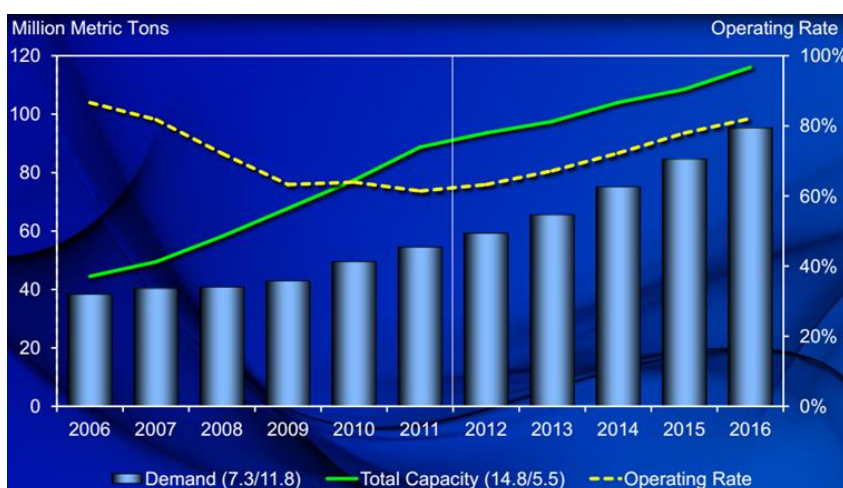
  It is used as reagent in many process like organic chemistry (elimination reaction). It is also used as solvent in many processes. It is also used for washing glass.

- *Antifreeze*

  Antifreeze is an additive that can alter the freezing and boiling points of the coolant in internal combustion engine that use water cooling. As the name implies, the main purpose of these additives is to prevent the liquid coolant from freezing, which can cause extensive engine damage. So methanol was used as reagent in the engine.

- *Waste Water treatment*

  Through a process known as "denitrification", water treatment facilities convert the excess nitrate into nitrogen gas which is then vented into the atmosphere, thus eliminating its ability to cause algal bloom in watersheds and block oxygen and sunlight from reaching marine life below the surface. Methanol is the most common organic compound used in denitrification, accelerating the activity of anaerobic bacteria that break down harmful nitrate [11].

- *Biodiesel*

  In the process of making biodiesel fuel, methanol is used as a key component in a process called transesterification – to put it simply, methanol is used to convert the triglycerides in different types of oils into usable biodiesel fuel. The transesterification process reacts methanol with the triglyceride oils contained in vegetable oils, animal fats, or recycled greases, forming fatty acid methyl esters (biodiesel) and the by-product glycerine. Biodiesel production continues to grow around the globe, with everything from large-scale commercial operations to smaller, backyard blenders mixing this environmentally-friendly fuel for everyday use in diesel engines [10].

1.6. Conventional process for methanol formation

1.6.1. Steam Reforming Process [12]

The process is endothermic which means heat must be supplied to the process for the reaction to proceed. The current commercial methanol synthesis technology is an energy intensive two-step process in which the first step is methane-steam reforming. In this first step, (shown below) a nickel base catalyst is used with an operating temperature range 500–1100◦C and an operating pressure range 15–30atm.

1ˢᵗ step:

CH₄ + H₂O ↔ 3H₂ + CO $\quad\quad$ ΔH $_{298\ K}$ = 206 kJ/mol (reaction 1)

CO + H₂O ↔ CO₂ + H₂ , $\quad\quad$ ΔH $_{298\ K}$ = − 41 kJ/mol (reaction 2)

Overall Reaction -

CH₄ + 2H₂O ↔ CO₂ + 4H₂ $\quad\quad$ ΔH $_{298\ K}$ = 165 kJ/mol (reaction 3)

The methane-steam reforming reaction (reaction 1), which is endothermic, is thermodynamically favoured by high temperature and low pressure. On the other hand, the water–gas shift reaction (reaction 2) is not pressure dependent and is favoured by low temperature (exothermic reaction). However, heat produced by the second reaction is never able to make up for the heat required for the first reaction and the overall reaction is endothermic. Thus, furnaces are required for additional heat input. Two-thirds of the operating costs of the overall process come from this first step. This product stream is then fed to the methanol synthesis stage (second step). The catalyst used in this step is a Cu/ZnO/Al₂O₃ catalyst (operating temperature range is 220–300∘C and the operating pressure range is 50–100atm). The two important reactions that occur within this stage, shown below, are exothermic.

2nd step :

CO + H₂O ↔ H₂ + CO₂ $\quad\quad$ ΔH $_{298\ K}$ = − 41 kJ/mol

CO₂ + 3H₂ ↔ CH₃OH + H₂O $\quad\quad$ ΔH $_{298\ K\ =}$ − 49.5 kJ/mol

Overall reaction -

CO + 2H₂ ↔ CH₃OH $\quad\quad$ ΔH $_{298\ K}$ = − 90.5 kJ/mol

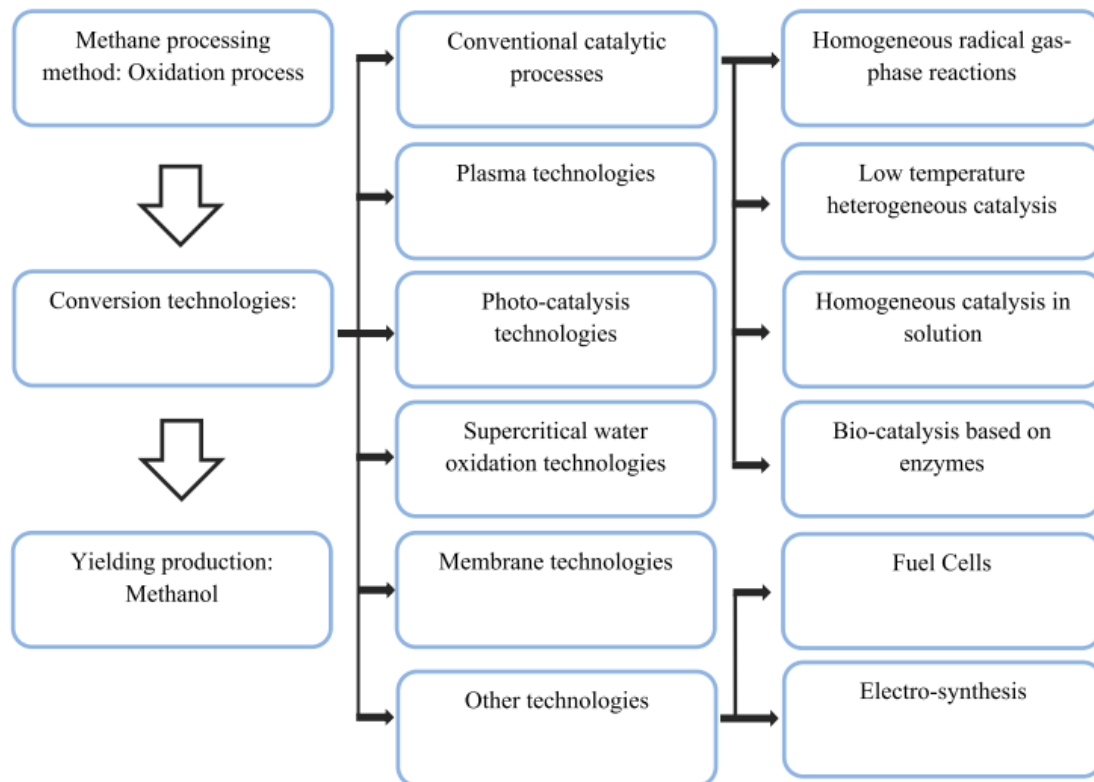**1.6.1.2. Other processes for methanol synthesis [13]**

Fig. 4. Diagram of diverse conversion pathways of methane to methanol.

1.7. Literature Survey

1.7.1. Thermal condition

Catalyst	Reactants	Condition (Temp/Pressure)	Selectivity (CH₃OH)	Reference
CuZnAl	$CO/CO_2/H_2$	$170^0C/3.0MPa$	67.93%	[14]
CuZnZr	$CO/CO_2/H_2$	$170^0C/3.0MPa$	88.06%	[14]
CuZnCe	$CO/CO_2/H_2$	$170^0C/3.0MPa$	80.60%	[14]
$Cu/ZnO/ZrO_2/Al_2O_3/SiO_2$	H_2/CO_2	$250^0C/5.0MPa$	99.72%	[15]
$Cu:Mn:Zn:CO/Cr_2O_3/K_2O_3$	$CO/CO_2/H_2$	$170^0C/1500psi$	79.8%	[16]
$CuO/ZrO_2(7)$	H_2/CO_2	$220^0C/1.7MPa$	67.0%	[17]
Pd/Ga_2O_3 Co-Precipitation $Pd(NO_3)_2$	H_2/CO_2	$523^0C/5.0MPa$	10.1%	[18]
Pd/ZnO imprignation $Pd(NO_3)_2$	H_2/CO_2	$523^0C/3.9MPa$	50%	[19]
Cu/Ga2O3/ZrO2	H_2/CO_2	$523^0C/2.0MPa$	75.59%	[20]

deposition precipitation				
Cu/Zn/Al/ZrO$_2$/ Co-precipitation	H$_2$/CO$_2$	513^{0}C/4.0MPa	47.20%	[21]

1.7.2. Plasma condition

Catalyst	Reactants	Condition (Temp/Pressure)	Selectivity (CH$_3$OH)	Reference
No Catalyst	CH$_4$/O$_2$	25^{0}C/1atm	30.0%	[22]
Nio/ZnO/CdO	CH$_4$/O$_2$	120^{0}C/1atm	34.1%	[22]
Cuo/ZnO/Al$_2$O$_3$	CH$_4$/O$_2$	DBD/25^{0}C/1atm	19% to 23%	[23]
Cu/ZnO/Al$_2$O$_3$	CH$_4$/O$_2$	DBD/25^{0}C/1atm	15% to 18%	[23]
Cu-Ni/CeO$_2$	N$_2$O/CH$_4$	DBD/25^{0}C/1atm	36.0%	[24]

1.8. Advantages of non-thermal plasma over conventional technique

As from the above discussion we can see that conventional process is two-step process as the steps increases the consumption of energy increases and it became economically less favourable. But with the use of non-thermal plasma it become one step process and reduces the overall production cost of methanol. Conventional process is highly endothermic means we have to provide energy for the process. Even pressure in conventional process is changed and It is very difficult to manage [25]. But in non-thermal plasma the temperature is actually the room temperature and the pressure is atmospheric pressure. Electric field is used as energy in case of plasma and it is less polluting. Overall economical yield in conventional process is very less but in non-thermal plasma yield is quite good. Overall process of formation of methanol in conventional process is very rigorous but in plasma its quite easy to handle with zero pollution [25].

CHAPTER 2
TECHNIQUES AND INSTRUMENTS

2.1. Introduction of Plasma

Plasma is often referred to as the fourth state of matter, an ionized gas [26]. The word "ionized" here to say the least means one or more electron(s) is or are not attached to molecule or an atom, turning them into ions that are positively charged [27]. Irving Langmuir (1928) first introduced the term plasma to the world. Plasmas are generated as a result of ionization of gases by application of either electric field, energetic beam or by adiabatic gas compression. Plasmas are a collection of charged and neutral species having overall zero electrical charge. Plasma have the following features: -

- ➢ Plasmas are capable of producing active species (e.g. ions, electrons, radicals, and atoms different wavelength photons and various excited species.) very high concentrations of energetic and chemically [27].
- ➢ Systems consisting of plasma generally do not attain thermodynamic equilibrium, thus forming chemically active species in large concentrations, simultaneously adjusting bulk temperature to near about room temperature.
- ➢ Energy density and temperatures of components of some plasma can exceed those of conventional.

2.2. **Types of plasma**

Based on type of reactors different plasma can be generated. On the basis of temperature variation of different constituents, there are two different types of plasma.

2.2.1. Thermal Plasma:

They are generally known as hot plasma in American and European literature and as low temperature plasma (in order to distinguish them from thermonuclear fusion plasma) in Russian literature. These plasmas are in partial local thermodynamic equilibrium (PLTE). This is because the low lying energy levels of atoms may be under populated, due to high radiative transition probabilities of these levels, resulting in a corresponding overpopulation of ground state. Hence it deviates from complete local thermodynamic equilibrium (CLTE). In thermal plasmas pressure exceeds 10 kPa and the electron and heavy particle temperature separates ($T_e > T_h$) [27].

Fig. 5. Thermal plasma

2.2.2. Non-Thermal Plasma

They are non- equilibrium plasma. They are also termed as "cold plasma". In contrast to thermal plasmas, non- thermal plasma operates at pressures of < 10 kPa. Unlike thermal plasmas non thermal plasmas have multiple temperature gradients between various plasma species. Energy is primarily delivered to electrons instead of molecules. Thus temperature of gas remains cold, whereas electrons gain energy and temperatures range from 10,000 K to 100,000 K (1-10 eV). Temperatures of heavy particles range from 300 K-1000 K. As temperature of the heavier species is low in this type of plasma, $T_h \ll T_e$. Hence, energetic electrons initiate reactions.
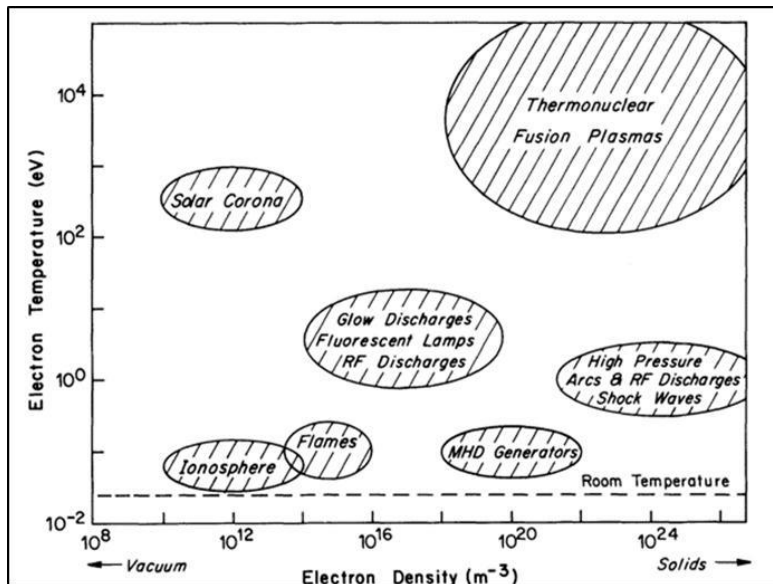

Fig 6. The range of pressure at which different plasma operates. [26]

2.2.2.1. Dielectric Barrier Discharge

18

Dielectric barrier discharges, also generalized as silent or barrier discharges. They can be operated with convenience, over a wide range of temperature and pressure. About the atmospheric pressure electrical breakdown occurs in many independent thin current films.

Dielectric barrier discharge (DBD) was first introduced by W. Siemens for the purpose of "ozonizing". Buss in 1932 noticed that the gap between electrode and insulated electrodes facilitate the breakdown of air in numerous individual tiny breakdown channels. Further studies were conducted on observation of Buss by Heuser. Tanka et al. Hirth. and Bagirov et al. These breakdown parameters were later on termed as microdischarges. DBD are recognized on the basis of the presence of insulating layer(s) in the path of current between metal electrodes with addition to the space of discharge. DBD configurations are of two specific types, i.e., cylindrical and planar, illustrated in figure below. At dielectric surface a channel of microdischarge covers a considerable surface area much greater than the diameter of the channel, thus in turn converting into a surface discharge [28].
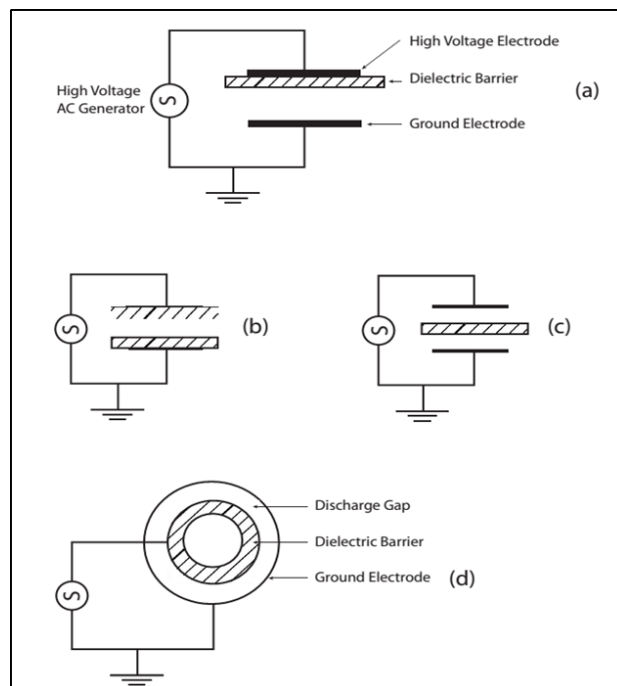

 Fig 7. Representation for the common layout of Dielectric Barrier Discharge; a, b,c-Planar, d-cylindrical[28].
.

2.2.2.2. Corona Discharge

Corona discharge refers to negative or positive electrical discharge caused due to ionization of surrounding gas to a conductor, for instance, a mineral surface, when electric field strength of exceeds a certain threshold value. Plasma is generated about the surface forming the ions, which disperse their charges to nearby areas having lower potential, or result in neutral molecules by their recombination. If the ionized zone keeps on growing instead of quenching, a continuous arc may result or a momentary spark may form. In a strong electric field region, a molecule or neutral atom in the medium, may undergo ionization, for example, a free electron or a positive ion can be created by the absorption of a photon. Separation of charged particles and their recombination is prevented by electric field around the surface. Henceforth electrons accelerate and electron/positive-ion pairs are formed from collision with rest of the neutral atoms. These then undergo the same processes creating a cascade of electrons [26].
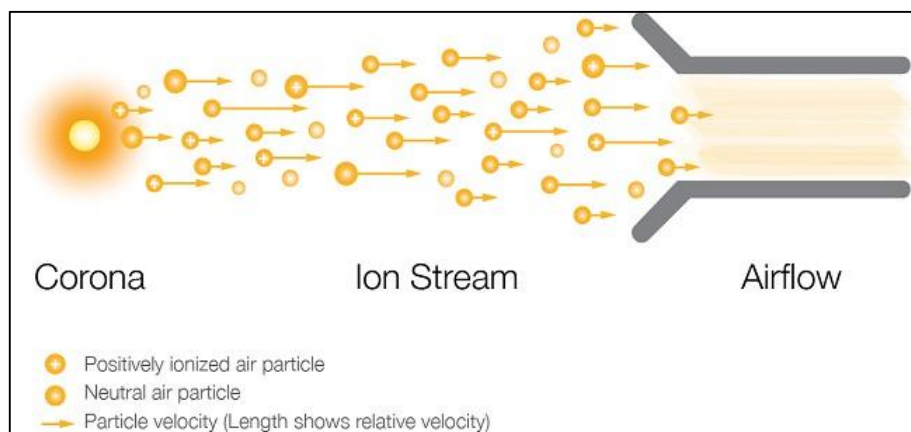

Fig 8. Ion generation and flow in corona discharge.

2.2.2.3. Radiofrequency Discharge

At low pressure conditions, radiofrequency plasma is profoundly cold and in non-equilibrium; less frequent electron–neutral collisions are while intensive cooling of gas by the walls occurs; as a result, Te >> T_0, similar to glow discharges. As a consequence of ion transfer and ionization frequencies the lower RF limit results. During a period of electromagnetic field oscillation sheaths and ion density in RF discharge plasmas can be usually considered to be constant. Therefore, RFs normally cross 1 MHz range (sometimes smaller); the most often used in industry is 13.6 MHz. Non-thermal RF discharges is categorized into low pressure, and those of moderate. In the moderate pressure discharges (1–100 Torr), the local electric field determines the electron energy distribution function (EEDF) and the characteristic system sizes are greater than electron energy relaxation length.

At low-pressure discharges EEDF is calculated by electric field distribution in the entire discharge and the discharge sizes is comparable to the electron energy relaxation length. Non-thermal RF discharges can be either inductively (ICP) coupled or capacitive (CCP) coupled. Low plasma resistance is required for effective coupling with the RF power supply.
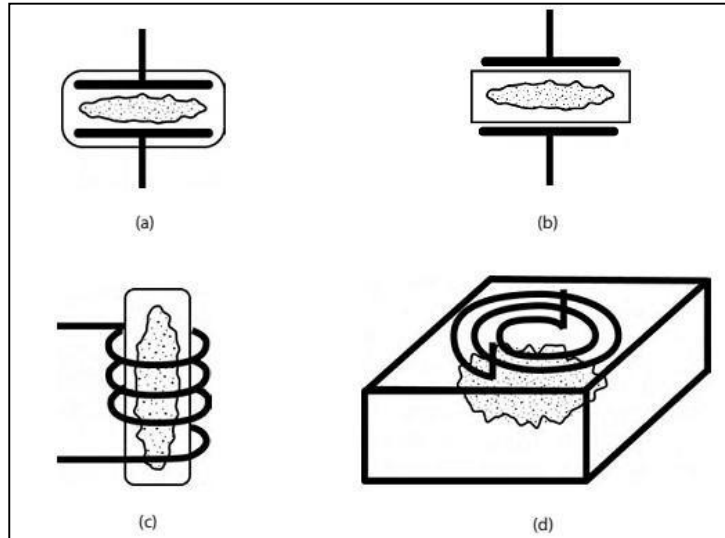

Fig 9. (a) and (b) are CCP whereas (c) and (d) are ICP; RF discharge

2.2.2.4. Glow Discharge Plasma

Glow discharge plasmas are generated by passing electric current through gases at low pressure. Two metal electrodes are present in a glass tube containing gas and potential is applied between them. As the applied voltage crosses or rather exceeds the breakdown voltage of the gas present in tube, it ionizes, turning into plasma. Thereafter it conducts electricity and glows with coloured light. When high voltage is applied accelerate rapidly towards the anode attaining a high velocity. Since one can relate kinetic energy to temperature, thus the electrons are hot as they reach high temperatures because of their low masses in cold gas molecules.
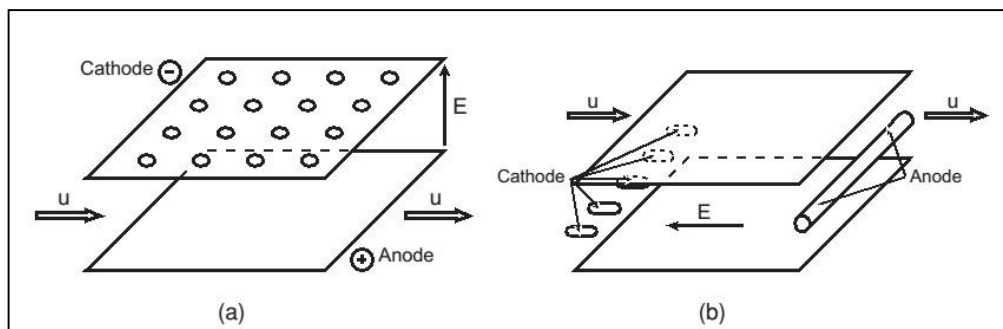
Fig 10. (a) organization of discharge flow in transverse manner; (b) organization of discharge flow in longitudinal manner. Glow discharge plasma

2.3. Commercial applications of plasma

The first noticeable contribution of plasma to the industrial sector was ozone synthesis from oxygen using silent discharge by Siemens in 1850. Plasma because of its diverse nature has turned out to be of prolific importance in a wide range of industrial applications and technological developments. Following are a list of plasma applications:

Chemical Synthesis

- Plasma spraying
- Diamond film deposition
- Ceramic Powders

Medicine

- Instrument sterilization
- Surface treatment

Surface treatment

- Ion implantation

Radiation Processing

- Water purification
- Seed germination

2.4. Gas Chromatography

The analysis of gas mixture was done using gas chromatography. The term chromatography in general refers to the separation of chemical mixtures into their respective pure components and is applicable for both liquid and gaseous samples. The GC (Shimadzu GC- 2014), equipped with a packed column (Hayasep A, 80/100 mesh, 3 m) and a TCD detector is used in the present experiment.t

2.5. XRD

The XRD pattern of prepared catalysts were collected on X'Pert PROP Analytical, Netherlands between $2\theta = 10^0 - 90^0$ at a scan rate of 0.01670 s^{-1} by using Cu Kα radiation (λ = 0.15418 nm).

2.6. SEM

A field emission scanning electron microscope (SEM- Zeiss Supra 40) was used to carry out the surface morphology analysis of the prepared catalysts.

2.7. TEM

The size and morphology of the nanoparticles were examined by a FEI model TECNAI-G-220 S-Twin TEM instrument.

2.8. OES

The emission spectrum was recorded for the discharge using an emission spectrometer (Princeton Instrument Action SpectraPro® SP-2300) having three different gratings (1200 g mm-1 with 500 nm Blaze, 600 g mm-1 with 750nm Blaze and 600 g mm-1 with 500 nm Blaze) utilizing an optical fibre to record the spectrum.

CHAPTER 3

EXPERIMENTAL SECTION

3.1. Introduction

The aim of this chapter is to illustrate the experimental setup utilized for the conversion of methane to methanol utilizing a DBD reactor. The key parameters for various calculation aspects are discussed below.

3.2 Experimental Setup

The experimental setup used for the present experiment is presented in Fig. 11. DBD consists of a quartz tube with an inner diameter of 20mm and outer diameter of 23mm. A stainless steel rod of 11mm diameter serves as the inner electrode. A SS mesh wrapped over the quartz tube acts as an outer electrode with discharge length of 11cm and discharge volume of 24mL. The inner electrode is connected to an AC high voltage source, whereas, the outer electrode is grounded through a capacitor (0.4 µF). The discharge was ignited by varying the AC high voltage in the range 16 to 22 kV at a fix frequency of 50 Hz. The gas flow rate was controlled with mass flow controllers (GFC-17, Aalborg, USA). An Agilent 34136A HV probe was used to measure the applied voltage and the charge-voltage (Q-V) signals wave forms were recorded with a digital oscilloscope (Tektronix TDS2014B). The energy dissipated in the discharge was calculated from the Q-V Lissajous figure. The GC (Shimadzu GC- 2014), equipped with a packed column (Hayasep A, 80/100 mesh, 3 m) and a TCD detector is used for the analysis of the outcomes from the plasma reactor. To calibrate the GC, several blank injections were given with the interval of 20 minutes. For each and every voltage 2 injections were given and the average was taken for the future calculation. The emission spectrum was recorded for the discharge using an emission spectrometer (Princeton Instrument Action SpectraPro® SP-2300) having three different gratings (1200 g mm-1 with 500 nm Blaze, 600 g mm-1 with 750nm Blaze and 600 g mm-1 with 500 nm Blaze) utilizing an optical fibre to record the spectrum. The conversion of the reactant, selectivity and yield of products, specific input energy (SIE), energy efficiency were calculated as follows:

$$CH_4 \; conversion \; (\%) = \frac{CH_4 \; converted \; (mmol/min)}{CH_4 \; input \; (mmol/min)} \times 100$$

$$Selectivity \ of \ H_2 \ (\%) = \frac{H_2 produced(mmol/min)}{2 \times CH_4 converted(mmol/min)} \times 100$$

$$Selectivity \ of \ C_2H_6 \ (\%) = \frac{2 \times C_2H_6 \ produced(mmol/min)}{CH_4 converted(mmol/min)} \times 100$$

$$Selectivity \ of \ CO_2(\%) = \frac{CO_2 \ produced(mmol/min)}{CH_4 converted(mmol/min)} \times 100$$

$$Selectivity \ of \ CO(\%) = \frac{CO \ produced(mmol/min)}{CH_4 converted(mmol/min)} \times 100$$

$$Selectivity \ of \ HCHO(\%) = \frac{HCHO \ produced(mmol/min)}{CH_4 converted(mmol/min)} \times 100$$

$$Selectivity \ of \ CH_3OH(\%) = \frac{CH_3OH \ produced(mmol/min)}{CH_4 converted(mmol/min)} \times 100$$

$$Yield \ (\%) = Selectivity \times \ CH_4 \ conversion(\%)$$

$$SIE \left(\frac{J}{ml}\right) = \frac{60 \times power(W)}{Total \ gas \ flow \ rate(\frac{ml}{min})}$$

$$Energy \ efficiency \left(\frac{mmol}{kj}\right) = \frac{CH_4 converted(mmol/min)}{discharge \ power(W)} \times \frac{1000}{60}$$

$$Total \ carbon \ Selectivity(\%)$$
$$= \frac{[CH_3OH] + [HCHO] + [CO] + [CO_2] + 2 \times [C_2H_6]}{CH_4 converted} \times 100$$
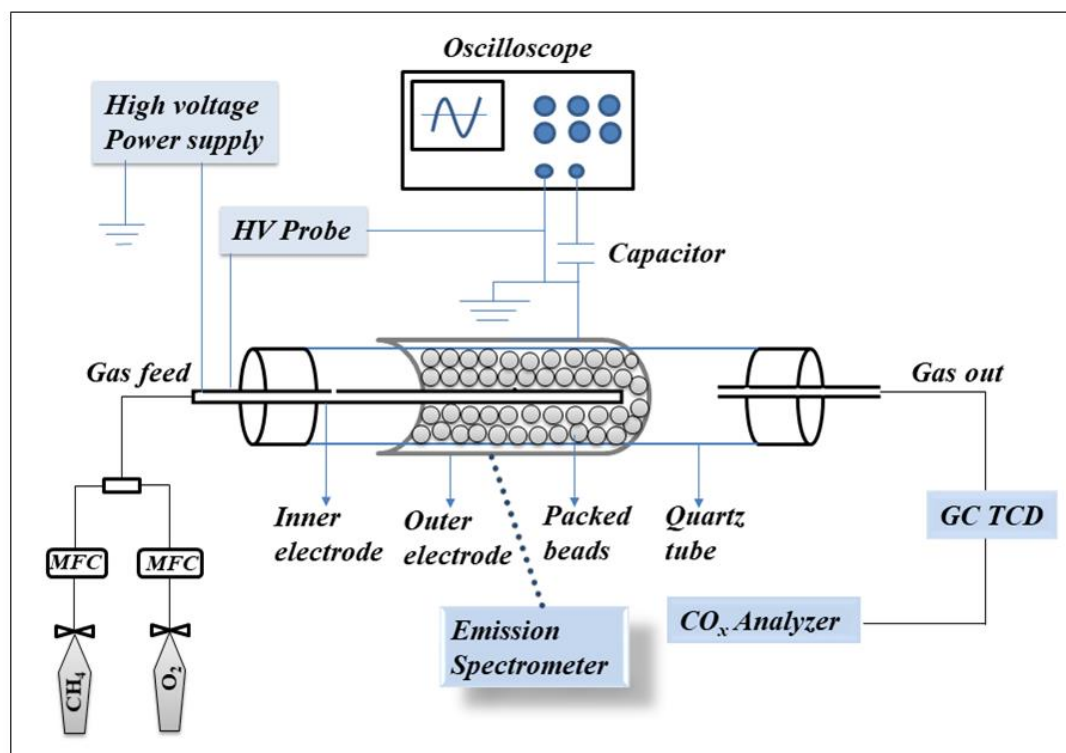
Fig. 11. Reactor set-up.

3.3. Catalyst preparation

5% CuO/γ-Al$_2$O$_3$ catalyst modified by ZnO, ZrO$_2$ and MgO were prepared by wet impregnation method with aqueous solutions of nitrates as metal precursors. Commercial γ-Al2O3 beads (Alfa Aesar) were used as the catalyst support. The support materials were pre-calcined at 500^{0}C for 2 h in air. The solution of the Cu(NO$_3$)$_2$.3H2O was impregnated on the supports. For the promoter modification, the ternary mixture of the two precursor solutions was impregnated on the supports. The catalysts were dried and subsequently calcined at 500^{0}C for 4hrs.

CHAPTER 4

RESULT AND DISCUSSION

4. Results and discussion

4.1. Non-catalytic Plasma MPOM reaction

4.1.1. Effect of gas feed ratio on reactant conversion and product distribution

It is known that the reactant gas feed ratio (CH_4: Air molar ratio) plays an important role on the conversion of CH_4, energy efficiency, product selectivity and yield of the products. Therefore, it is essential to optimize the appropriate CH_4: Air ratio for higher reaction efficiency. Fig. 12 shows that CH_4 conversion increases with decreasing CH_4: Air molar ratio in each power step at a fixed total flow rate (30 mL/min), which suggests that the higher content of oxidant (zero air) in the reactant mixture leads to the improvement of CH_4 conversion. The highest CH4 conversion was achieved ~ 9.3% at CH_4: Air molar ratio of 1.5:1. A decrease in the CH_4: Air molar ratio resulted in more oxygen active species available in plasma zone to react with methane molecules, which leads to the higher reactant conversion.
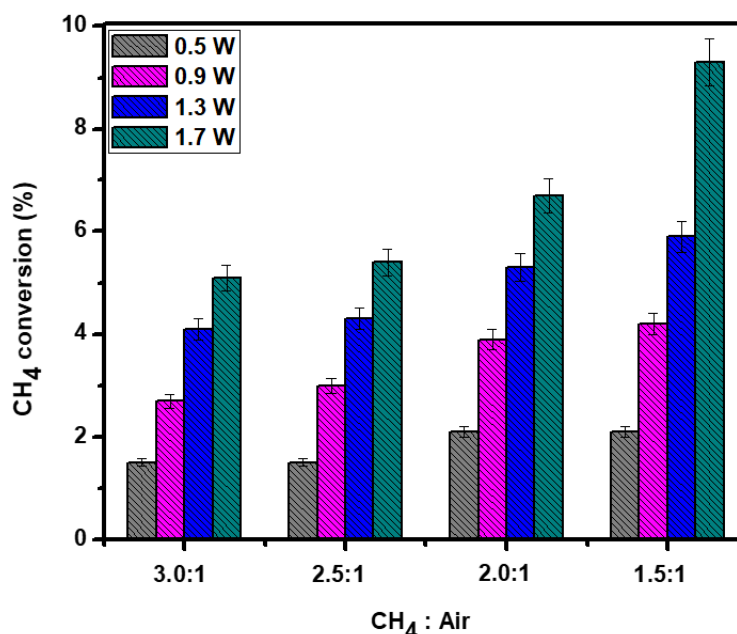

Fig. 12. Effect of CH_4: Air molar ratio on CH_4 conversion. (Total flow rate 30 mL/min, frequency: 50 Hz).

Fig. 13 shows that the product distribution was also affected significantly with feed gases ratio variation. A high yield of the products could be obtained at lower CH_4: Air molar ratio. As the

CH$_4$: Air molar ratio decreases from 3 to 1.5, the CH$_3$OH and HCHO yield approaches around 4 times increment while 2 times increase of CO yield was observed. An improvement of H$_2$, C$_2$H$_6$ and CO$_2$ yields were also achieved with higher air concentration. As shown in Fig. 13a, b and c, at higher CH$_4$: Air molar ratio H$_2$ and C$_2$H$_6$ formation dominates over other oxygenates (CO, CO$_2$, HCHO, CH$_3$OH). This is may be due to that at higher feed gases ratio there was not enough atomic oxygen concentration to react with the available CH$_4$ active species. On the other hand, the higher oxygen content in the reactant mixture suppresses the recombination of active CH$_x$ species which results the lower yield of hydrocarbon formation. Again, one of the main considerable product in methane partial oxidation is syn-gas (H$_2$-CO mixture) with a maximum 1.9% CO and 1.8% H$_2$ yield. Moreover, it was observed that CH$_4$: Air molar ratio has a notable effect on the H$_2$/CO molar ratio in gas products. As seen in Fig. 131d, the H$_2$/CO ratio decreases from 3 to 1.9 as moving from the CH$_4$: Air molar ratio 3:1 to 1.5:1. This is because of the higher production of CO over the H$_2$ produced in the 1.5:1 (CH$_4$: Air) reaction outcome, which in other way improves the CH$_3$OH production.
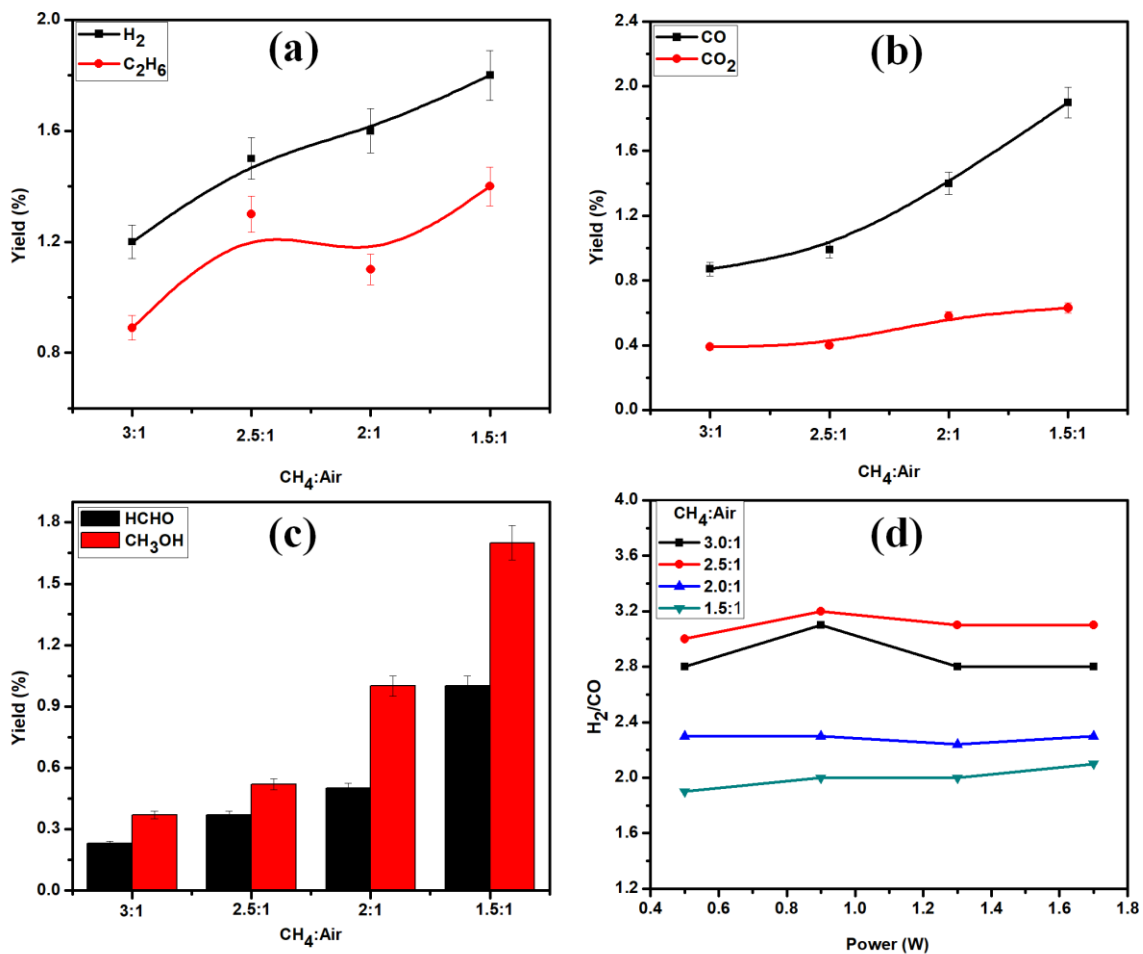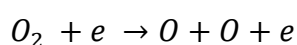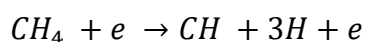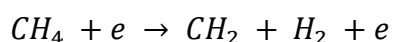

28

Fig. 13. Effect of feed gases ratio (CH_4: Air) on products yield. (a) H_2, C_2H_6 (b) CO, CO_2 (c) HCHO, CH_3OH (d) H_2/CO ratio. (Total flow rate: 30 ml/min; Frequency: 50 Hz).

4.1.2 Effect of SIE on product selectivity

Electronic and chemical processes of partial oxidation of methane in the plasma start with the generation of filamentary micro discharges in the dielectric barrier discharge and continue with ionization, excitation and dissociation of methane and zero air by electron impact reactions.

$$CH_4 + e \rightarrow CH_3 + H + e$$

$$CH_4 + e \rightarrow CH_2 + H_2 + e$$

$$CH_4 + e \rightarrow CH + 3H + e$$

$$O_2 + e \rightarrow O + O + e$$
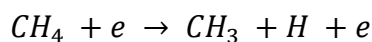
The active species (CH_3, CH_2, CH, H, O, OH) interact with each other and further recombine to give different products like H_2, CO, CO_2, H_2O, HCHO, CH_3OH and higher hydrocarbons. In DBD, the specific energy input (power/flow rate) determines the generated electron density inside the plasma reactor and furthermore influences the subsequent chemical reactions. To understand the effect of SIE on the reactant conversion and products selectivity, the power was varied between 0.5 to 1.7 W at a fixed CH_4: Air ratio of 1.5:1 with a total flow rate of 30 mL/min. Fig. 14 presents that both the CH_4 conversion and products selectivity increase with SIE rise which implies that selectivity of each product is very sensitive to the input power as the intensity of plasma streamers grows well with input power. The increment of methane conversion rate almost follows a linear trend with increasing order of SIE, which was consistent with most relevant reports [29, 30, 31]. Fig. 14 also illustrates that at lower SIE region the maximum product selectivity comes from H_2, CO, CO_2 and C_2H_6 while at higher SIE region HCHO and CH_3OH selectivity dominates with the dropdown of other products selectivity. The highest CH_3OH selectivity of 18.4% was obtained at the highest SIE of 3.4 J/mL applied in present experiment. In addition, CO_2 selectivity does not alter in that extent which in turns improves the HCHO selectivity at higher SIE.
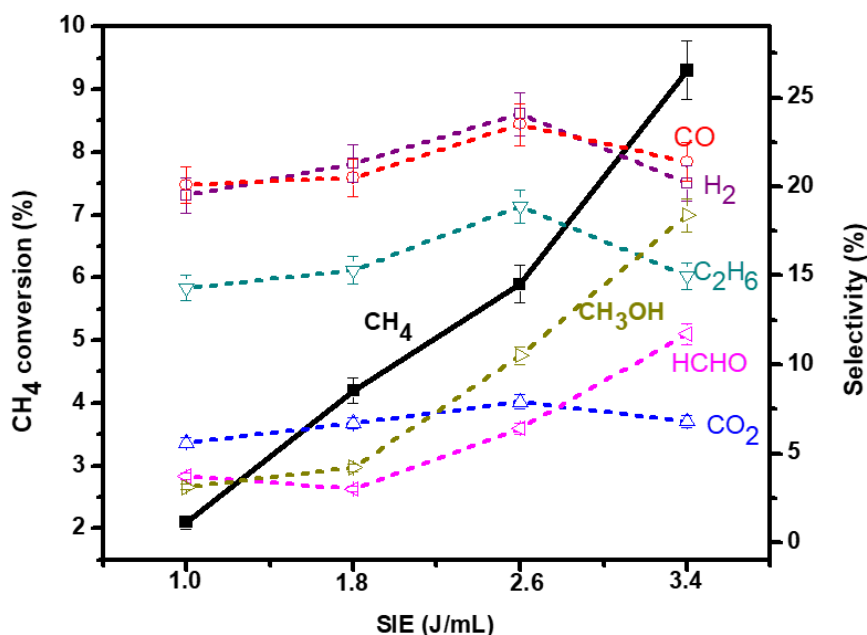
Fig.14. SIE variation on CH_4 conversion and products selectivity. (Total flow rate: 30 mL/min; CH_4: Air = 1.5:1).

4.1.3. *Total carbon selectivity and energy efficiency*

A gradual increase both in total carbon selectivity and energy efficiency with decreasing CH_4: Air molar ratio was clearly evidenced by fig. 15. This increase was due to the improved random collision among the high energetic electrons and the active species produced in higher air content reactant mixture. The oxygenates (CO, CH_3OH and HCHO) contribute most for the carbon selectivity at 1.5:1 ratio system while, in other cases C_2H_6 covers the maximum carbon selectivity for higher methane contained system. A superior energy efficiency (~ 0.73 mmol/kJ) was obtained from 1.5:1 (CH_4: Air) molar ratio. In comparison of 3:1 ratio system ~ 27% increase in energy efficiency was observed in 1.5: 1 ratio system at constant power of 1.7 W.
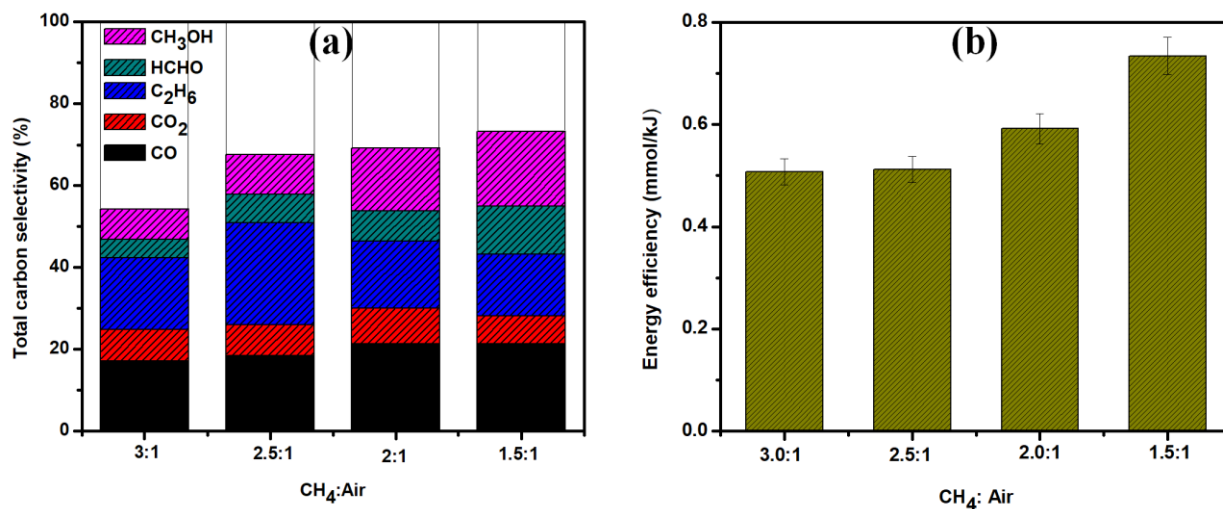
Fig. 15. Influence of air content variation on (a) total carbon selectivity and (b) energy efficiency; (Total flow rate: 30 mL/min; Power: 1.7 W; frequency: 50 Hz).

4.2. Plasma catalytic methane partial oxidation to methanol

4.2.1. Catalyst characterization

4.2.1.1. X-ray diffraction analysis

Fig.16 shows the XRD pattern of the prepared catalysts. The XRD pattern of the γ-Al_2O_3 support shows three major diffraction peaks placed at $2\theta = 37.3^0$, 46.1^0, 66.5^0 corresponding to the (110), (202) and (214) planes of crystalline γ-Al_2O_3 (JCPDS-893072). All the catalysts show a strong diffraction signal characteristic of CuO species at $2\theta = 37.4^0$ [32]. Three weak diffraction peaks of the CuO which actually look like humps, also appear at $2\theta = 32.4^0$ (110), 38.9^0 (200) and 61.5^0 (-113) respectively in catalyst CA. However, the modification of the promoters (ZnO, ZrO_2 and MgO) can make these diffraction peaks weaken or sometimes disappear. Therefore, it can be proposed that the introduction of promoters influences the formation of amorphous CuO species with high extent of dispersion. The presence of ZrO_2 in CZrA catalyst can be confirmed by the appearance of two weak diffraction peaks of ZrO_2 at $2\theta = 24^0$ (011) and 48.9^0 (-212). But no diffraction signals were assigned to the ZnO and MgO species in the XRD pattern of CZnA and CMgA catalysts. It is possible because of the introduced promoter amount is too low and may be the promoter species are dispersed in the amorphous state.
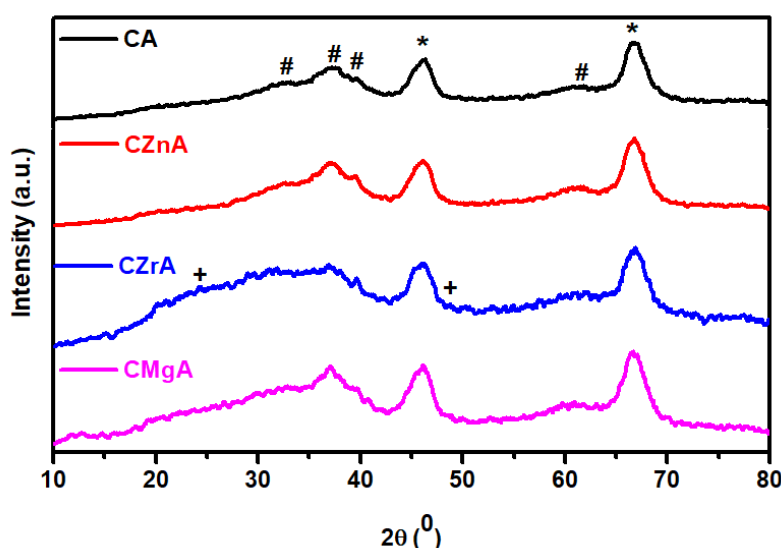

Fig.16. XRD pattern of the prepared catalysts. (# = CuO, * = Al_2O_3, + = ZrO_2).

4.2.1.2. SEM and EDS analysis

31

Fig. 17 presents the surface images of the prepared catalysts. It also shows that there is no significant difference among all the catalysts structure. Though all the particles on the surface of the catalysts have some irregular shape, but considering the surface roughness, CZrA and CMgA possess comparative smoother catalytic surface. Moreover, it can also be said that the promoter modification can lead to the improvement of the particle dispersion all over the catalyst surface. The elemental composition of the samples was determined by EDS analysis.
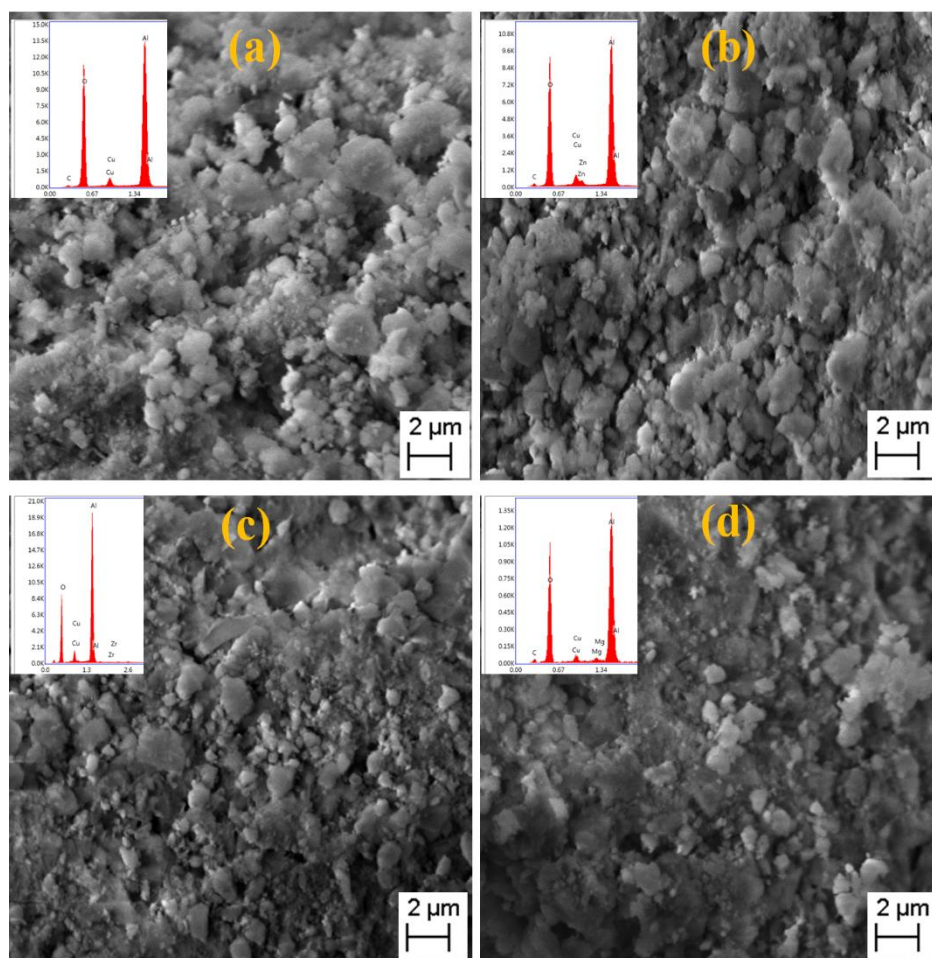

Fig. 17. SEM images and EDS spectra of the prepared catalysts. (a) CA (b) CZnA (c) CZrA and (d) CMgA.

4.2.1.3. TEM analysis

The TEM analysis resulted in Fig. 18 where the image of CA (Fig. 8a) reveals the fibrous nature of γ-Al_2O_3 support with black agglomerated dots of CuO crystallites. But the promoter modification (ZrO_2) makes the CuO crystallites more dispersed all over the catalyst surface and the average crystallite sizes around 15-20 nm as shown in Fig. 18c. Moreover, higher magnification image of CZrA catalyst (Fig. 8d) shows two kinds of periodicity of lattice fringes with d-spacing of 0.254 nm and 0.232 nm, which are compatible with the (-111) and (111)

planes of CuO respectively. The SAED pattern of the CuO crystallite conveys different planes of CuO (Fig. 18b) which were mostly not appeared in XRD due to very low percentage of CuO presented in the prepared catalysts.
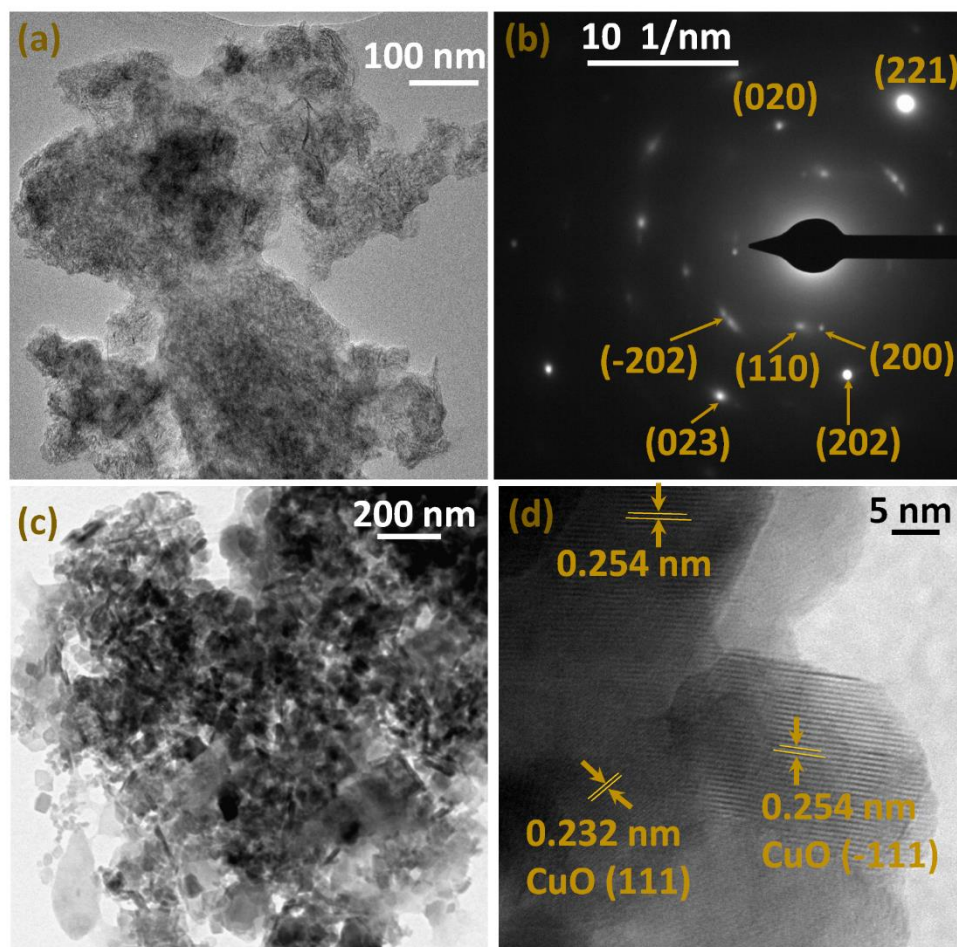

Fig. 18. HR-TEM images of the catalysts. (a) CA (b) SAED pattern of CuO in CA (c) TEM images of CZrA (d) lattice fringes in CZrA catalyst.

4.2.1.4. Emission spectroscopy analysis

The optical emission spectroscopy technique was performed to identify the active species generated inside the plasma discharge reactor during the partial oxidation of methane with zero air. The emission spectra of the discharges corresponding to without catalyst and combination of plasma-catalyst system followed by promoter modified catalyst was also measured. Resulted spectrum (Fig.19) shows various peaks of active species like NO, CO, CO^+, CH, CO_2, OH, O_2, N, N^+, N_2^+, H_2 and O_2. Generally, in non-equilibrium plasma the chemical reactions are initiated with the fast electron ionization process of the reactant gases. In the UV range, specially from 280 nm to 400 nm, the major emission bands are of CO, CO_2, OH and CH active species. A weak band of N_2^+ at 376 nm (due to B $^2\sum_u^+ \rightarrow$ X $^2\sum_g^+$ transition) comes from air

discharge in plasma, while a weak peak of NO at 250 nm was appeared. At 297 nm (B $^3\Pi^+ \to$ A $^3\Pi$) and 380 nm two bands of the CO were found, which are typically for CO containing discharges. A sharp peak of the OH radical at 357 nm due to $^3\Pi \to {}^3\Sigma$, (0,0) transition and a weak OH peak at 308 nm due to the A $^2\Sigma^+ \to X^2\Pi$ transition confirm the formation of liquid products (CH_3OH, and H_2O). There is one intense CH peak was observed at 315 nm which was ascribed by the C $^2\Sigma \to X$ $^2\Pi$ (1,1) and (0,0) transition with addition of one weak peak at 391 nm (B $^2\Sigma \to X$ $^2\Pi$). The CO_2 emission peaks were appeared at 337, 353, 370 and 375 nm wavelength respectively. But at higher wavelength (400-800 nm), there are many unidentified peaks arise which are mostly due to the impurity in the gases. Two CO bands at 520 nm (B $^1\Sigma \to$ A $^1\Pi$) and at 450 nm (D $^3\Delta \to$ A $^3\Pi$) were located in the spectrum and becomes more
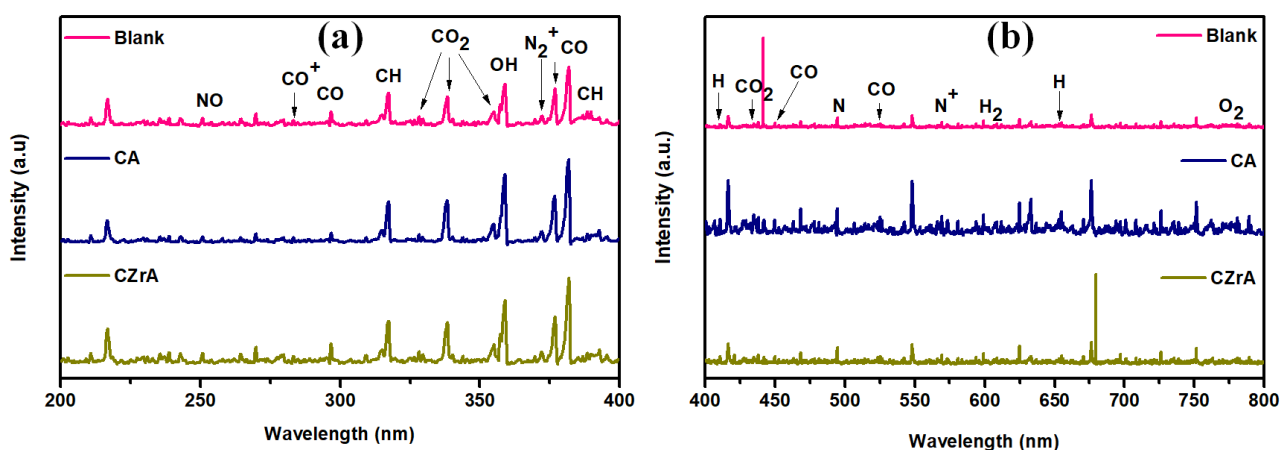
dominant on addition of catalyst on plasma discharge. Same happens when both the catalysts (CA and CZnA) combined with plasma, imparts higher intensity in the bands appeared for H at 655 nm and 410 nm respectively.

Fig. 19. Optical emission spectroscopy (a) wavelength at UV region, (b) wavelength at visible region (applied voltage 20 kV, grating: 600 glue at 500 nm).

4.2.2. Physical and electrical discharge characteristics of plasma packed catalysts

Fig. 20 points out the change in the shape of Lissajous figure on integrating catalysts with DBD plasma at constant power of 1.7 W. The area of the Lissajous figures in turn gives the information about the charge/power dissipated in the discharge. From Fig. 20c it can be deduced that the plasma catalyst combination imparts higher magnitude of charge- transfer per half cycle compare to mere plasma system. The order of dQ follows like CZnA> CZrA> CMgA> CA> plasma. This observation indicates that the catalyst integration on plasma affects the discharge behavior from typical filamentary micro discharge to a combination of limited filamentary discharge and a dominant surface discharge on the catalyst surface.

34

The physical properties of the catalysts are summarized in table 1. N_2 adsorption-desorption resulted the BET surface area of CuO/ γ-Al_2O_3 (208 m^2/gram) possess lower surface area than that of support γ-Al_2O_3 (224 m^2/gram). It indicates that the introduced cupper species occupy the inner surface of the support during impregnation process. BET surface areas of the other catalysts are also listed in table 1 which follows the decreasing order of CZrA> CZnA> CA> CMgA. Following results convey that the introduced metal oxide promoters (CZrA, CZnA) do not alter the surface area that much while, MgO addition further decreases the surface area. Therefore, it can be proposed that ZrO_2, ZnO modification lead to the improvement on the dispersion of cupper species over the catalyst surface area through suppressing the interaction between CuO and support, which further prevents the migration of metal cupper species into support structure [32].
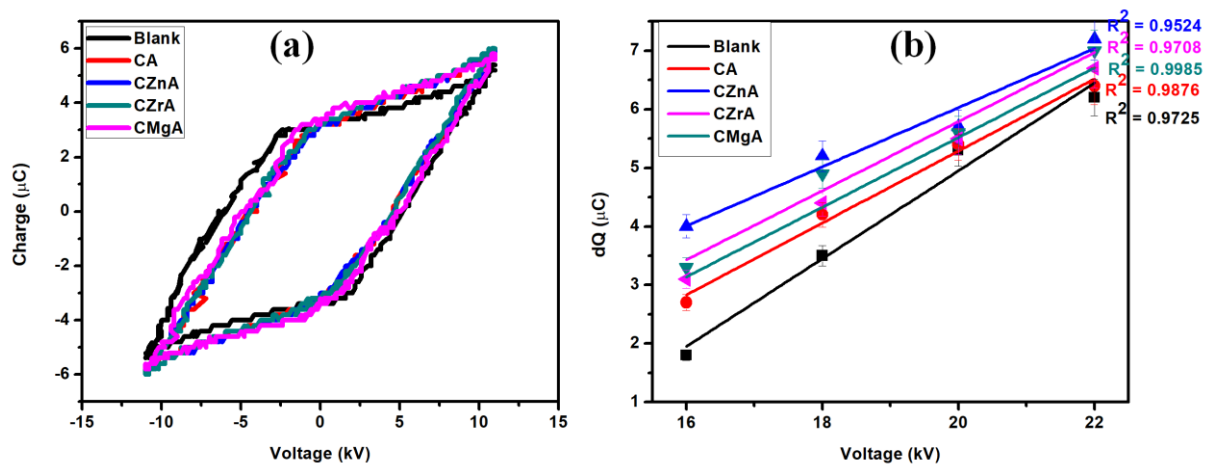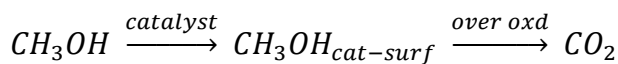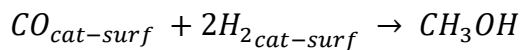

Fig. 20. (a) Lissajous figure of mere plasma and plasma-catalyst systems at constant power. (b) Charge-transfer per half cycle of different systems vs applied voltage. (Total flow rate: 30 mL/min; CH_4: Air = 1.5:1, Frequency: 50 Hz).

Table 1. Physical and discharge characteristics of the catalysts.

Packed catalyst	Surface area (m^2/gram)	Power (W)	Breakdown voltage (kV)	Charge-transfer per half cycle (μC)
Blank	-	1.7	5.6	6.2
CA	208	1.7	4.5	6.4
CZnA	209	1.7	4.6	7.2
CZrA	211	1.7	4.4	7.0
CMgA	204	1.7	4.7	6.7

4.2.3. Effect of catalysts on MPOM

Generally, in the plasma-catalyst system, the first step of the process is reactants activation by high energy electron impact which produces several active species (CH_3, CH_2, CH, H, O, OH) followed by a second step reaction where a heterogeneous reaction takes place on the external surface of the catalysts. Fig. 21. presents the catalyst performance on the methane partial oxidation to methanol. Compared to the non-catalytic plasma reaction, combination of plasma-catalyst system gave reliable increment on both CH_4 conversion and CH_3OH selectivity. Previously, the non-catalytic system (CH_4: Air = 1.5:1) produced dominant syn-gas (H_2 and CO) over the CH_3OH and HCHO, where in presence of catalysts both the H_2, CO selectivity decrease and simultaneously methanol selectivity increases as shown in Fig. 21b, c and d. Therefore, it can be said that the adsorbed syn-gas on catalyst surface further converted into methanol. CZrA catalyst also makes the point strong by producing highest methanol selectivity through the maximum syn-gas conversion. CO_2 selectivity also increases with catalyst addition which may be due to the further over oxidation of adsorbed liquid (CH_3OH, HCHO) on catalyst surface.

$$CO \xrightarrow{catalyst} CO_{cat-surf}$$

$$H_2 \xrightarrow{catalyst} H_{2_{cat-surf}}$$

$$CO_{cat-surf} + 2H_{2_{cat-surf}} \rightarrow CH_3OH$$

$$CH_3OH \xrightarrow{catalyst} CH_3OH_{cat-surf} \xrightarrow{over\ oxd} CO_2$$

$$HCHO \xrightarrow{catalyst} HCHO_{cat-surf} \xrightarrow{oxd} CO_2$$
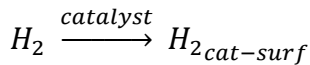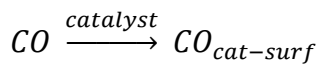
In case of CMgA catalyst, MgO addition decreases the catalyst surface area which further lowers the CuO particles dispersion as a result of the bigger cupper species. These bigger particles provide low activity on adsorbing and activating H2 and CO, which is disadvantageous to CH_3OH synthesis. But, the lower surface area of CMgA rather helps in HCHO production over the CO_2 formation.

 The conversion of CH_4 mostly affected by the SIE input as well as with catalysts integration on DBD. From the data presented at table.1 it can be seen that at constant power (1.7 W), break-down voltage of the catalysts decreases while on the other side dQ values increase gradually in comparison of mere plasma system. These two results support the improved CH_4 conversion

by the plasma-catalyst systems. The highest CH_4 conversion of ~11% obtained from CMgA catalyst which is around 22% increment compared to blank.

The highest methanol selectivity of 28.3% obtained from CZrA catalyst while CZnA provides the maximum HCHO selectivity of ~25%. According to the above characterization it can be deduced that the improvement on catalytic performance towards MPOM is mostly attributed to the higher Cu dispersion over the higher catalyst surface area, adsorption capacity of H_2 and CO after the promoter modification. Literatures also support the fact that the addition of ZnO increases the dispersion of Cu and acts as a reservoir for atomic hydrogen spilling on the Cu surface to promote the hydrogenation process [33, 34, 35]. In one side, when a catalyst integration improves the oxygenates selectivity, there is hardly positive contribution towards higher hydrocarbon formation as the C_2H_6 selectivity remarkably decreases compared to only plasma system. Generally, the hydrocarbon formation takes place due to the radical recombination in plasma zone and this radical recombination may be effective if there is no adsorbate materials in the plasma zone which is favoured to the catalyst free plasma region. Therefore, it can be said that the presence of catalyst inside the plasma favours fragmentation reactions between methane and oxygen active species over the recombination reactions.
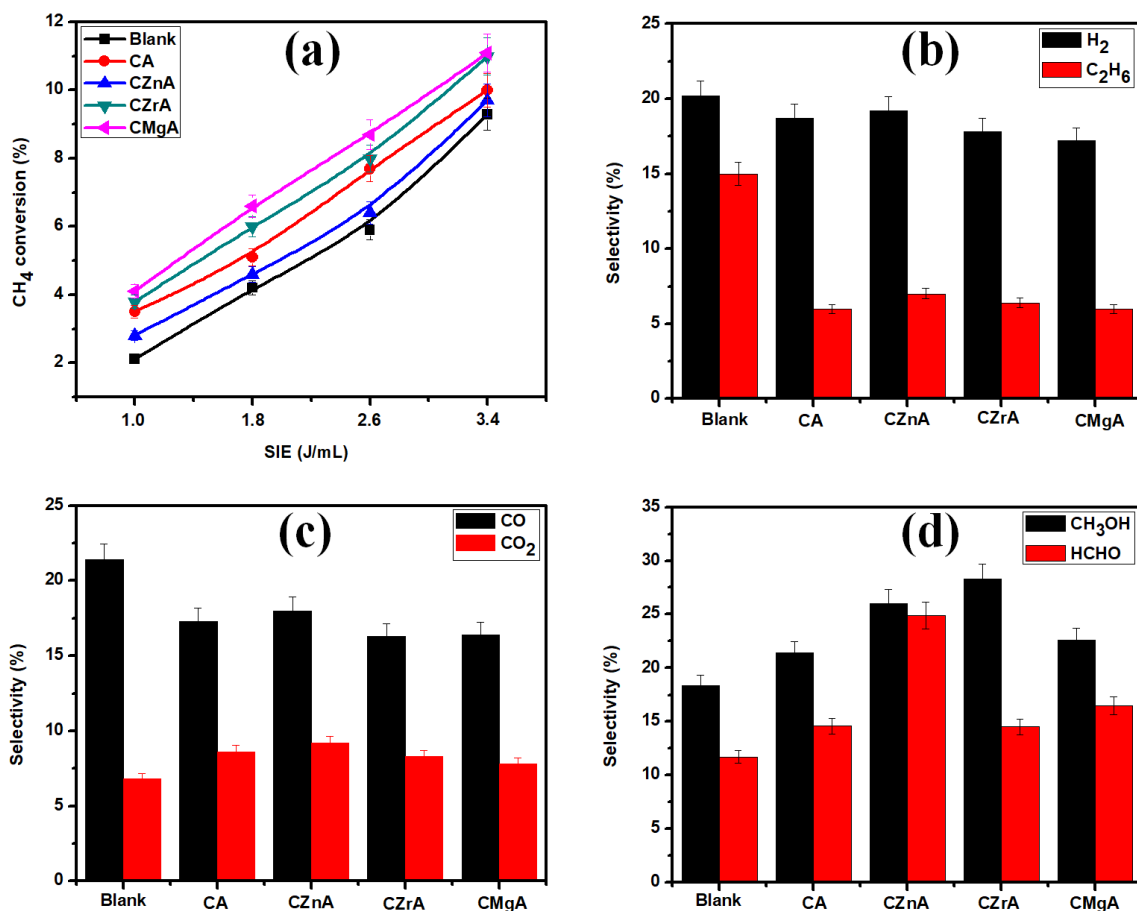
Fig. 21. Effect of catalysts on MPOM. (a) CH_4 conversion (b) H_2, C_2H_6 selectivity (c) CO, CO_2 selectivity (d) CH_3OH, HCHO selectivity. (Total flow rate: 30ml/min; CH_4: Air = 1.5:1; Frequency: 50 Hz).

4.2.4. *Total carbon selectivity and energy efficiency*

The improved energy efficiency and total carbon selectivity on catalyst introduced plasma system were observed in Fig. 22. Though all the catalysts (CA and CMgA) are not highly efficient to improve the total carbon selectivity but, ZnO and ZrO_2 addition in CuO/γ-Al_2O_3 show better performance in this regard. The highest carbon selectivity of ~85% was obtained from CZnA catalyst which was mostly attributed to the HCHO and CH_3OH selectivity.

Present experiment also results that the synergistic effect from the combination of plasma and catalysts effectively enhances the energy efficiency of the plasma MPOM. Compared to the mere plasma system (0.734 mmol/kJ) an increment of ~50% in the energy efficiency was observed when 5% CuO/MgO/Al_2O_3 was packed in the plasma zone. MgO addition gives the maximum value of energy efficiency due to its highest CH_4 conversion.
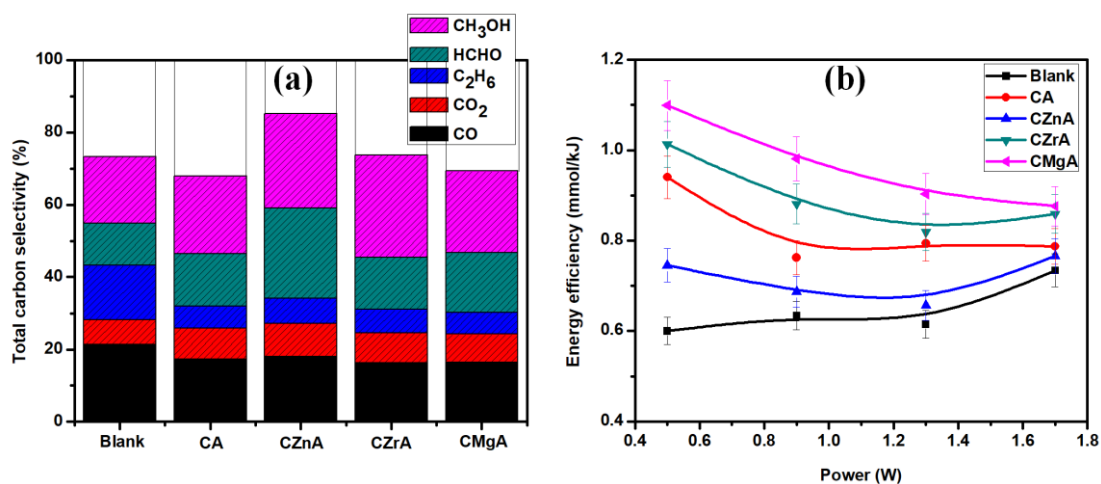
Fig. 22. Effect of catalysts on (a) Total carbon selectivity (b) energy efficiency. (Total flow rate: 30 mL/min; CH_4: Air: 1.5:1, Frequency: 50 Hz).

Conclusion

The plasma catalytic methane – air conversion to methanol was investigated in DBD reactor at ambient condition. Typical results indicated that the input power and oxidant concentration both has a marked influence on the CH_4 conversion and products selectivity. The maximum methanol selectivity of ~18% obtained from CH_4: Air = 1.5:1 ratio. Moreover, the catalysts integration on plasma led to the higher CH_4 (11%) conversion and CH_3OH (~28%) selectivity than a non-catalytic plasma process. CZnA catalyst shows maximum liquid selectivity while, ZrO_2 addition in CuO/Al_2O_3 improves CH_3OH selectivity specifically.

References-

1. Yuya Kajikawa, Junta Yoshikawa, *Technological Forecasting & Social Change,* **2008**,75, 771–782

2. *Int. J. Environ. Res. Public Health* **2018**, *15*

3. Kowalewicz, *A. Combustion systems of high-speed piston I.C. engines*, **1984,** 207, (Elsevier, Amsterdam)

4. James Hansen, Makiko Sato,*Department of Earth Science, University of California, Santa Barbara*, **2006**

5. Kirschke, S. et al. *Three decades of global methane sources and sinks*, **2006**, 6, 813–823.

6. Methane's Role In Climate Change, *92 Issue 27*

7. Gerhard K. Heilig,**1994**, 16, 109–137

8. Coal conversion and CO2 utilization, *China Coal Research Institute*; **2011**, 09

9. Pellegrini LA, Soave G, *Applied Energy*, **2011**, 88:4891–7

10. Mårten Larssona, Stefan Grönkvista, *Energy Procedia*, **2015**, 24, 1875 – 1880

11. *Journal of Engineering Science and Technology*, **2013**, 8, 578 – 587

12. David W. Larkin∗, Lance L. Lobban, *Catalysis Today*, **2001**, 71, 199–210

13. Z. Zakaria, S.K. Kamarudin, **2016**, 65, 250-261

14. Tang Xiao-bol, Noritatsu Tsubaki1, *J Fuel Chem Techno*, **2014**, 42(06), 704–709

15. J.Toyira,b, R. Miloua, M. Nawdali, *Physics Procedia*, **2009**, 1075–1079

16. Alvin B. Stiles, Frank Chen, *Ind. Eng. Chem. Res.*, **1991**, 30, 811-821

17. R.A. Koeppel et al., *Applied Catalysis*, **1992**, 84, 77-102

18. T. Fujitani, M. Saito, Y. Kanai, T. Watanabe, *Applied Catalysis*, **1995**, 125, 199–202.

19. N. Iwasa, H. Suzuki, M. Terashita, *Catalysis Letter*, **2004**, 96, 75–78.

20. X.-M. Liu, G.Q. Lu, Z.-F. Yan, *Applied Catalysis*, **2005**, 279, 241–245.

21. X. An, J. Li, Y. Zuo, Q. Zhang, Catalysis Letter, **2007**, 118, 264–269.

22. Mamoru Okumoto, B. S. Rajanikanth, *IEEE transactions on industry applications*, 34,**1998**

23. Antonius Indarto, Jae Wook Choi, *IEEE transactions on plasma science*, **2008,** 36

24. Sk. Mahammadunnisa, K. Krushnamurty, Ch. Subrahmanyam, *Catalysis Today*, **2005**, 256, 102–107

25. David W. Larkin, Liming Zhou, Lance L. Lobban, and Richard G. Mallinson, *Ind. Eng. Chem. Res.*, **2001**, 40, 5496-5506

26. *An introduction to the theory of astrophysical, geophysical, and laboratory plasma, Peter A. Sturrock*, Cambridge University Press, **1994**, ISBN- 0521448107

27. Plasma chemistry, Alexander Fridman, ISBN-13 978-0-521-84735-3

28. David W. Larkin, Liming Zhou, Lance L. Lobban, and Richard G. Mallinson, *Ind. Eng. Chem. Res.*, **2001**, 40, 5496-5506

29. G.B. Zhao, S. John, J.J. Zhang, L. Wang, *Chem. Eng. J.*, **2006**, 125, 67–79

30. L. Chen et al., *Chemical Engineering and Processing*, **2009**, 48, 1333–1340

31. L.M. Zhou, B. Xue, U. Kogelschatz, B. Eliasson, *Plasma Chem. Plasma Phys.*, **1998**,18 375–392.

32. H. Ren et al.,*Journal Of Industrial And Engineering Chemistry,* **2015**, 28, 261–267

33. R. Burch, S. E. Golunski, M. S. Spencer, *J. Chem. Soc*, **1990**, 86, 2683-2691

34. J. D. Grunwaldt, A. M. Molenbroek, N. Y. Topsøe, *„Journal of Catalysis*, **2000**,194, 452-460.

35. G. C. Chinchen, K. C. Waugh, D. A. Whan, *Applied Catalysis*, **1986**, 25, 101-107.